Characterization of an Electro-thermal Microactuator with Multi-lateral Motion in Plane

C. H. Pan*, Y. K. Chen**, C. L. Chang**

*National Chin-Yi Institute of Technology, Taiwan, ROC
Fax: 886-4-23930681, E-mail: pancs@chinyi.ncit.edu.tw
** National Yunlin University of Science & Technology, Taiwan, ROC

ABSTRACT

We present a new electro-thermal microactuator to have multi-lateral motion in plane by only varying voltage potentials at the contact pads. To extend the operating function, the larger operating range or multi-mode switch, relay and optic tweezer can be achieved. For focusing on the characterization of the microactuator, the finite element software ANSYS is used to perform the electro-thermo-mechanical behaviors of the microactuator to demonstrate the feasibility of the design principle. Design parameters (including structural dimensions, selective doping and thermal boundary conditions) significantly influencing the performance are studied. According to the analysis results, it is found that low voltages (0~7V) are required to achieve displacements in microns with the operating temperatures below 300℃. The optimal structure can be obtained by varying geometric dimensions and resistivity of the beams to meet the proper performance.

Keywords: microactuator, electro-thermal, multi-lateral motion

1 INTRODUCTION

Although there are different types of microactuators, most of them perform one-direction motion in plane (parallel to the substrate) or out-of-plane (vertical to the substrate). Only some of them may have bi-direction motion [1-5], which are achieved by mechanically coupling an array of microactuators, by assembling 3D microactuators or by utilizing bi-stable effect. Very few microactuators can perform multi-direction motion in plane or out-of-plane by itself. In 2001, Pan and Hsu [6] proposed an electro-thermally and laterally driven microactuator, which had bilateral motion in plane. It was symmetric combination of two basic microactuators presented by Pan and Hsu in 1997 [7]. In 1992, Guckel et al. [8] presented an electro-thermal microactuator which operating principle is based on unequal thermal expansion of the structure with different beam widths. This paper will present a new microactuator that combines the traits of the two basic microactators proposed by Pan and Guckel, respectively, to achieve multi-lateral motion in plane. The design principle is based on: (1) the asymmetrical thermal expansion of the beams with different lengths and cross sections and (2) the selective doping of varying resistivity within the structure.

2 DESIGN CONCEPT

A schematic diagram of the new microactuator is shown in Figure 1. Figure 2 displays four operating modes (mode (a), (b), (c) and (d)) of the microactuator with its current path and effective heating beams, and the deformed shapes of simulation are presented also. In mode (a), both inside hot beams (we call them hot beam II) are effective heating beams. The two tips of microactuator will move outward simultaneously. In mode (b), at another input voltage mode, both outside hot beams (we call them hot beam I) are effective heating beams. The two tips will move inward simultaneously. In mode (c), the hot beam (I) on the right side and the hot beam (II) on the left side are effective heating beams. Both two tips will move to the left. Finally, in mode (d), the hot beam (I) on the left side and the hot beam (II) on the right side are effective heating beams. The two tips will move to the right.

3 FINITE ELEMENT MODELING

The commercial finite element code ANSYS is used to perform coupled-field analysis of the electro-thermo-mechanical behaviors by modeling the microactuator as a 3-D shape structure. The solid45 mechanical element type and solid69, solid70 thermal element types are used. Besides, the coupled field element type solid5 is used also. Figure 3 displays the 3D solid model and meshing model of the microactuator for the entire structure (including the suspended beams, the anchor layer and the substrate). In simulation, the material properties that are temperature dependent, such as the thermal expansion coefficient, thermal conductivity, resistivity, Young's modulus and convective film coefficient, are treated as constant values here for the low operating temperatures (< 300℃).

4 CHARACTERIZATION

4.1 Optimal Structure Approach

In order to ensure that the microactuator can realize the four operating motion and to gain maximum lateral displacement at the same input voltage but with maximum temperature below 300℃, some design rules motivate the structure design focusing on the optimal lengths of cold beam (Lc), hot beam II (Lh2), flexure beam (Lf) and the optimal width of bridge beam (Wb). Other design dimensions are choose and fixed at Lh1=500 μm, Lb=50 μm, Wt=10 μm, Wc=24 μm, Wt=10 μm, W=4 μm, h=2 μm, g=3 μm, air gap=3 μm, contact pads=80 μm x 80 μm and the Silicon substrate referred as a thicker block.

Furthermore, the influence of selective doping (varying resistivity) of the beams is also considered. Figures 4, 5 and 6 show the variations of themaximum displacement of the microactuator with different dimensions of the cold beam (Lc), hot beam II (Lh2), flexure beam (Lf) and the bridge beam (Wb). Figure 7 shows the influence of varying resistivity in heavily doped area on the performance. According to the above results, it is found that the geometrical parameters and varying resistivity have a strongly influence on the performance of the microactuator, and thus the optimal structure can be obtained by varying the dimensions and resistivity of the beams to meet proper performance.

4.2 Thermal Boundary Condition Effect

After optimal structure approach, one optimal dimesions (Lh1=500 μ m, Lb=50 μ m, Lh2=150μm, Lc=250μm, Wb=30μm, Lf=70μm, Wt=10 μ m, Wc=24 μ m, Wt=10 μ m, W=4 μ m, h=2 μ m, g=3 μ m, air gap=3 μ m, pads=80 μ m x 80 μ m) is adopted for inquiring into the effect of thermal boundary conditions. The steady state temperature distribution and the tip displacements of the microactuator under various applied voltages, different operating modes and different thermal boundary conditions are simulated in this section. By feasible assumption, under low operating temperatures(< 300℃), the heat dissipated through conduction and radiation to the ambient can be neglected as compared to the heat loss by conduction to the substrate via the pads/anchors (Here the substrate is referred as a heat sink with a large thermal mass at the ambient temperature) [9-12]. Besides, the conductive heat loss through thin (2~3 μ m) air gap to the substrate seems to be not neglected [12,13]. Here, various trenches (air gaps) under the suspended beams are included in the numerical analysis. Furthermore, because of the ratio of surface area to volume of a solid increases with diminishing size as the structure size reduces, the convection heat loss from the surfaces, especially the large surface areas of cold beam, bridge beam and pads, are accounted for in the model. The results are summarized from figure 8(a)-(c). Gathering the results of the figures, it is indicated that the thermal boundary conditions really play an important role in the performance of the microactuator. Although the performance of the microactuator may be affected by various thermal boundary conditions, the multi-lateral motions are going quit well and can be controlled accurately at an invariant environment. However, for widely and accurately utilizing the microactuator, comprehensive heat transfer analysis (such as the temperature dependence of thermophysical and heat transfer properties, heat loss by radiation) under a high temperature range should be studied further.

5 CONCLUSIONS

This paper presents a new electro-thermal microactuator to have four operating motions in plane by only varying voltage potentials at the contact pads. According to the characterization, it is found that only low input voltages (0~7V) are required to achieve displacements in microns with the operating temperatures below 300℃. The parameters that influence the design limitation and performance of the microactuator have been studied. It is revealed that the optimal structure can be obtained by varying dimensions and resistivity of the beams to get proper performance of the microactuator. The performance of the microactuator may be affected by various thermal boundary conditions, but the multi-lateral motion behaviors are going quit well and can be controlled accurately at an invariant environment. To extend the operating function, we can manipulate the microactuator to generate a versatile path motion in plane by varying operating modes and with various input voltages, that will enlarge applications in micro devices with larger operating range or acting as a multi-mode switch, relay or optic tweezer.

REFERENCS

[1] Jaecklin V. P., C. Linder, N. F. de Rooij, and J. -M. Moret, Sensors and Actuators A 39, pp.83-89, 1993.

[2] Matoba H, Ishikawa T, Kim C J and Muller R S IEEE Transducers'94, pp 45-50, 1994.

[3] Yeh R., Kruglick E. J. J. and Pister K. S. J., J. Micromech. Syst., 5, 1, pp.10-17, 1996.

[4] Comtois, J. J. and Bright, V. M., Sensors and Actuators A **58,** pp.19-25, 1997.

[5] Que L, Park J S and Gianchandani Y B, J Microelectromech. Syst., 10, 2, pp.255-262, 2001.

[6] Pan C. S. and Hsu W., J. of the Chinese Society of Mechanical Engineers, 22, 1, pp.71-78, 2001.

[7] Pan C. S. and Hsu, W., J. Micromech. Microeng., **7,** pp.7-13, 1997.

[8] Guckel, H., Klein, J., Christenson, T., Skrobis, K., Landon, M., and Lovell, E. G., IEEE Solid State Sensor and Actuator Workshop, pp.73-75, 1992.

[9] Fedder G. K. and Howe R. T., *Proc. IEEE Micro Electro Mechanical System Workshop* pp.63-68, 1991

[10] T ai Y. C., Mastrangelo C. H., Muller R. S., *J. Appl. Phys.* 63 (5) 1 pp.1441-1447, 1988.

[11] Lin L and Pisano A P, *ASME DSC-32* pp 147-163, 1991.

[12] Lin L., Chiao M, *Sensors and Actuators* A55 pp.31-41, 1996.

[13] Mankame N D and Ananthasuresh G K, *J. Micromech. Microeng.* 11 pp. 1-11, 2001.

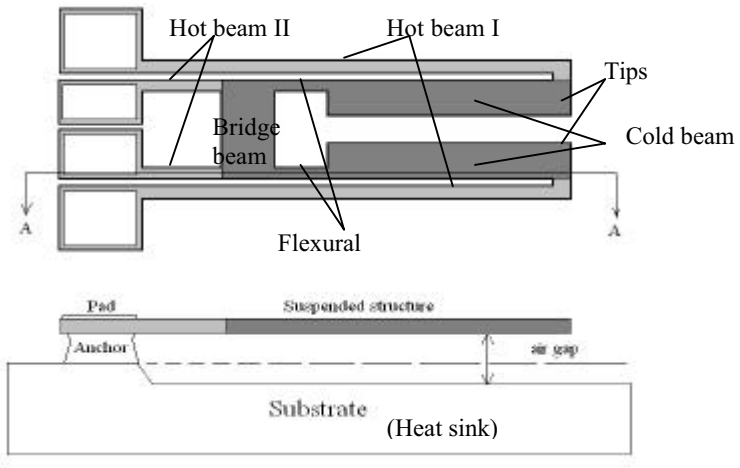

Figure 1: the schematic diagram of the new microactuator

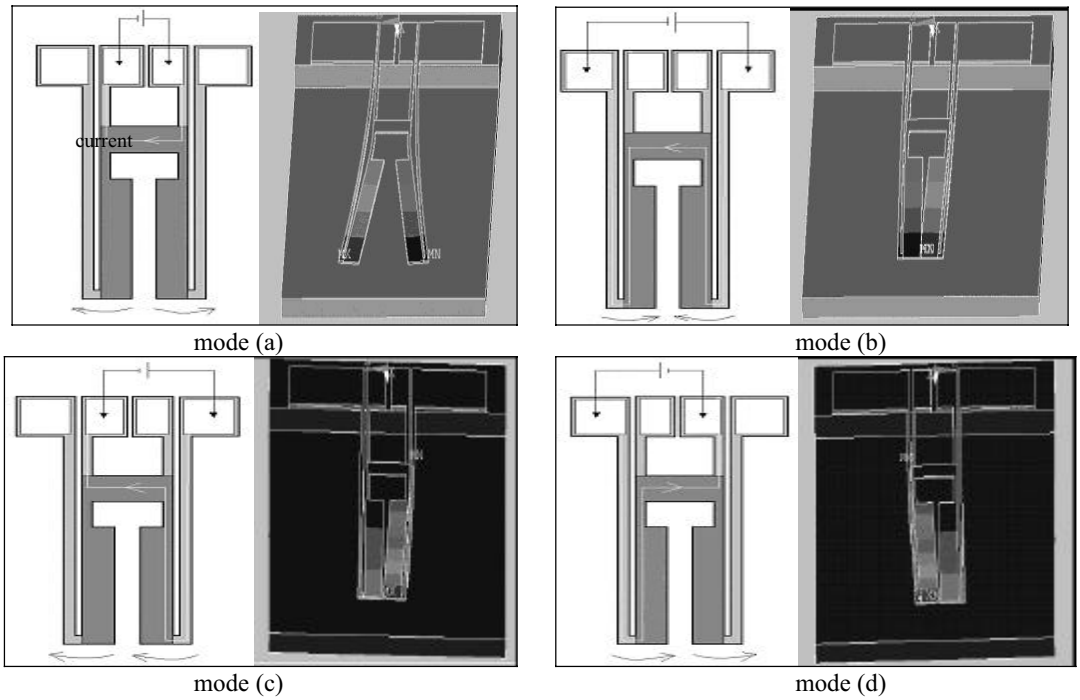

mode (a) mode (b)

mode (c) mode (d)

Figure 2(a)-(d): four operating motions of the microactuator with its input voltage mode

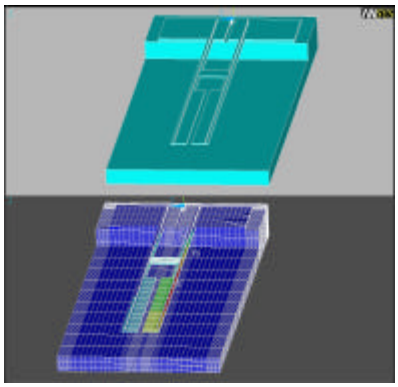

Figure 3: 3D solid and meshing models for finite element analysis

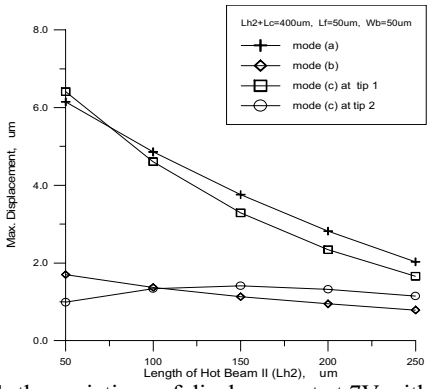

Figure 4: the variations of displacement at 7V with various dimensions of the hot beam II (Lh2) and cold beam (Lc)

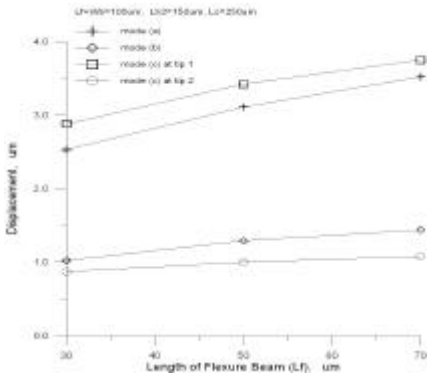

Figure 5: the variations of displacement at 7V with various dimensions of the flexure beam (Lf) and bridge beam (Wb)

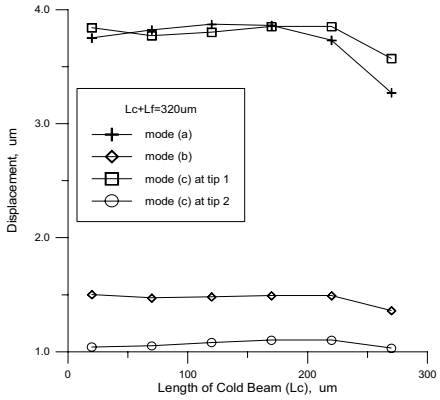

Figure 6: the variations of displacement at 7V with various dimensions of the flexure beam (Lf) and cold beam (Lc)

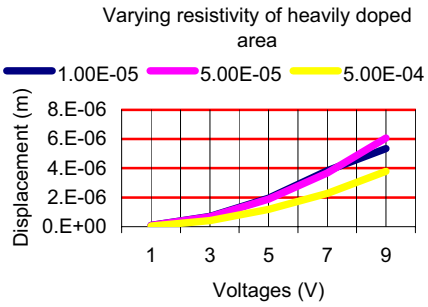

Figure 7: the influence of varying resistivity on performance (mode (c) as example)

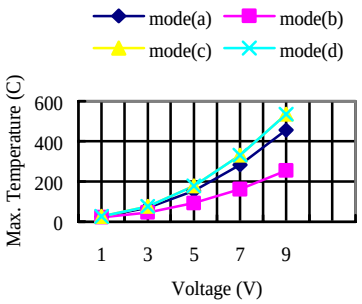

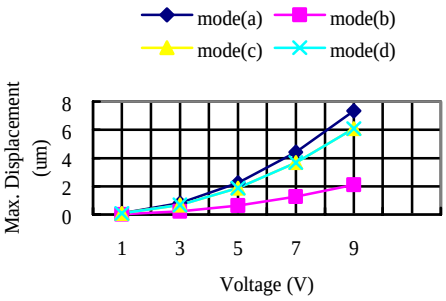

(a) only conduction

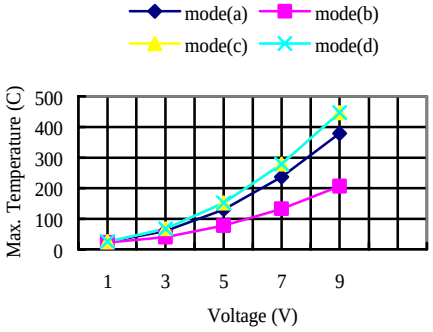

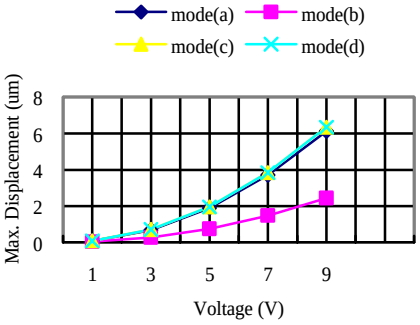

(b) conduction and convection (hf=50 [W · m^{-2} · ^{o}C^{-1}])

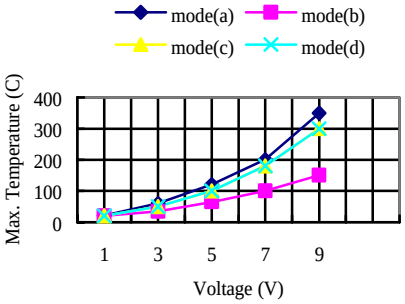

(c) conduction, convection and conduction to the substrate via air gap (3 μ m)

Figure 8(a)-(c): the influence of different thermal boundary conditions on the temperature and displacement of the microactuator